SUPERSATURATION EVOLUTION AND FIRST PRECIPITATE LOCATION IN CRYSTAL GROWTH IN GELS; APPLICATION TO BARIUM AND STRONTIUM CARBONATES

M. PRIETO, L. FERNÁNDEZ-DIAZ, L. and S. LÓPEZ-ANDRÉS

Dpto. Cristalografía y Mineralogía, Universidad Complutense, 28040 Madrid, Spain

Supersaturation is not enough to interpret nucleation behavior in crystal growth in gels. The explanation for the first precipitate location needs complementary crystallization criteria. The experimental testing of both mass-transfer and pH evolution is the background to establish rigorous hypotheses. From these data, the actual distribution of free ions, ionic associations and supersaturation throughout the gel column may be found. In the case of nucleation of strontianite and witherite crystals, although the critical supersaturation conditions remain necessary, a second concept, the "equality range" of the reagent concentrations, has to be introduced to account for observations. With these dual conditions, the behaviour of the described gel-diffusion system is correctly reproduced. The significance of pH evolution is also experimentally shown. Nucleation density and growth mechanisms are finally explained on the base to supersaturation rate and kinetic roughness.

1. Introduction

In crystal growth in gels, volume mass-transfer occurs by diffusion. Consequently, theoretical treatment of mass-transfer have usually been based on Fick's diffusion law analytic solutions. However, in such analytic approaches, diffusion systems and source reservoirs are respectively considered semi-infinite and inexhaustible, whereas actual systems are finite. Such procedures are, therefore unsuitable for testing many kinds of theoretical predictions and particularly those concerned with the location of precipitates. In fact, in crystal growth in gels, the experiments are often described by attending to the initial concentration of the reagent's mother solutions: any quantitative mention of concentration evolution is absent.

Henisch and García-Ruiz [1] have described a microcomputer implementation which allows one to solve Fick's diffusion equation by numerical methods. This treatment is a suitable procedure for finite systems with different configurations. However, the systems they have worked with are hypothetical and several assumptions have been made for the sake of simplificity: complete ionization, concentration-independent diffusion constant, etc. Therefore this approach is a good instrument in an interpretative way, but not in a quantitative one.

Prieto et al. [2] deal with laboratory experiments specifically designed to test the mass-transfer in a U-tube arrangement, where two counter-diffusing reagents meet to generate a sparingly soluble reaction product. From experimental data these authors show that the commonly made simplifications to model the mass-transfer may lead to remarkable deviations from reality. Moreover, following these authors, the supersaturation evolution throughout the gel column must be evaluated attending to actual complexity factors. For instance, the pH evolution and the presence of both free ions and ionic associations in solution must be considered.

However, mass-transfer quantification is not enough to predict the first precipitate location. Appropriate criteria have to be available for such an assessment. Therefore the establishement of rigorous "crystallization criteria" is the second problem of the crystal growth in gels theory.

Regarding this problem, it is usually been considered that crystallization begins when the reagent's concentration product exceeds a critical value. If this criterion were correct, then the first crystallization would always take place at the point of the gel column where the concentration product shows a maximum. Therefore, if the reagent's diffusion coefficients are equal and concentration-independent (complete ionization and other simplifications are assumed in this asseveration), the first precipitate must always form in the middle of the diffusion column, even for different initial concentrations of mother solutions. This prediction stands, however, in contradiction to experimental facts [3], meaning that either the simplifications introduced are not possible or a complementary hypothesis is necessary.

Henisch and García-Ruiz [4] consider the case of an U-tube arrangement. Following these authors, the critical product condition is insufficient for a stocastically controlled system, like nucleation in a gel. That condition suggests, for instance, that the reagent concentration ratio is irrelevant, which is absurd for a system of limited particle mobility. Hence, these authors propose a second condition, the "equality range" of reagent concentrations, stated in equivalents: the nucleation probability should be very small, unless the ratio of the concentrations of both reagents exceeds a certain minimum value. Such a condition must be considered in relation with frequency of arrival of growth units to nucleus, in accordance with the preexponential factor of the nucleation rate expression [5].

However, up to now, no complete experimental checking of this hypothesis has been carried out. Such is the aim of this paper that deals with laboratory experiments which have been specifically designed to interpret the first precipitate location. Mass-transfer and pH experimental testing allows us to know the concentration and supersaturation profiles in the gel column when crystallization begins. So, it is possible to check whether the "equality range" condition is fulfilled in the first crystallization zone.

The study is applied to growth of barium and strontium carbonate crystals in a U-tube gel system.

2. Experimental

Mass-transfer testing was carried out in a double diffusion-reaction system (fig. 1). In such a system, two reagents, $BaCl_2$ or $SrCl_2$ and Na_2CO_3, diffuse through a silica gel column (9 mm diameter and 280 mm long) to meet and generate $BaCO_3$ or $SrCO_3$ as a reaction product. Silica gel was prepared by the acidification of a Na_2SiO_3 solution (Merck, Sp.Gr.: 1.059 g/cm^3; pH 11.2) with HCl (1N) solution until the desired pH level (5.5 in all the experiments) was obtained. The source reservoirs were filled with 8 cm^3 of $BaCl_2$ or $SrCl_2$ (0.5M, 0.3M and 0.1M) and Na_2CO_3 (0.5N, 0.3N and 0.1N) solutions. The temperature of experiments was 25 °C.

Mass-transfer testing was carried out by reactant diffusion during previously stated periods of time (200, 300, 400, 500, 850, 1000, 1500, 2000, 2500, 3000, 3500 and 4000 h). After the diffusion period, the gel columns were sliced, and the gel slices (10 mm long) were chemically analyzed.

Chemical analysis of barium, strontium and sodium was done by atomic absorption Spectrophotometry (an UNICAM SP90 absorption Spectrophotometer was used). The detection limit was 0.006 μg/ml for strontium, 0.05 μg/ml for barium and 0.001 μg/ml for sodium. The total amount of carbon in the gel slices was measured by means of a C–N–S elemental analyser (Carlo Erba Na-1500) with a detection limit of 0.001 wt%. However, the effective control of chemical determination accuracy is done by the slicing process precision: a gel column is easily deformable and consequently an error up to 1% for gel slice weight may be expected. Therefore the error

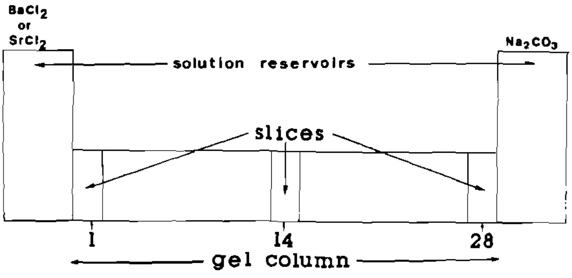

Fig. 1. Experimental gel growth system.

margin for concentration values is 1% concentration dependent.

Chemical constituent concentrations, measured in this particular way, must be referred to the "effective water" [2] per gel volume unit in order to obtain the actual concentrations of intersticial solutions. It is also worth noting that the so-obtained concentration values are total values for each entire slice, by removing the concentration gradient inside each slice. Therefore the concentration graphics throughout the gel column are bar graphics, on the understanding that the actual concentration gradient would be done by the bar enveloping.

The gel pH evolution was also studied. With this object in view, silica gel was prepared by adding pH universal liquid indicator (Merck) to the Na_2SiO_3 solutions. As in all other experiments reported here, the gel pH was adjusted to 5.5. Therefore the gel column exhibits initially an homogeneous colouring. The subsequent pH evolution, as a result of the reagent diffusion, clearly shows a colour banding in the gel column. From this banding the pH profiles may be found for different diffusion times and different concentrations of mother solutions.

The nucleation and growth behaviour of $SrCO_3$ and $BaCO_3$ was studied by attending to nucleation density, experimental induction time (the time taken for the first crystallites to appear under magnification ×500) and location of the first crystallization. The morphology of the crystals was monitored in situ by optical microscopy. Some crystals were recovered from the gel, and their surface topography was observed by scanning electron microscopy. Identification was made by X-ray diffraction (powder method with Cu Kα radiation).

3. Mass-transfer and pH evolution

In finite systems, mass-transfer follows a different outline from the theoretical forecast for semi-infinite systems. The total concentration values of strontium (mmol/l) through the diffusion column are represented in fig. 2a. The slices are numbered from 1 to 28, the first being the nearest to the $SrCl_2$ mother solution. Different curves correspond to different diffusion times. Fig. 2b represents the same kind of data for barium. Table 1 shows the corresponding numerical values.

The graphics are similar to the one obtained by Prieto et al. [2] for calcium. Curve morphologies continuously change in time. The curve corresponding to a short diffusion period (300 h) is the only one that shows an aspect similar to that expected, from a theoretical point of view, for a semi-infinite system with infinite solution reservoirs. For longer diffusion times the curves are sigmoidal: the concentration decreases in the initial extreme, whereas it increases in the final extreme as diffusion time passes by. This means a continuous change in the edge conditions that

Table 1
Strontium and barium concentration profiles for different diffusion times; mother solutions: 0.5M $SrCl_2$ or $BaCl_2$

Slice No.	Strontium (mmol/l)			Barium (mmol/l)		
	Diffusion time (h)			Diffusion time (h)		
	300	1000	2000	300	1000	2000
1	226	178	171	206	273	230
2	148	165	166	170	254	225
3	106	152	162	138	233	213
4	76	136	149	107	209	198
5	53	118	140	64	165	181
6	35	97	119	43	130	160
7	24	83	108	30	105	139
8	17	68	91	20	83	120
9	11	55	72	15	72	95
10	7	48	68	8	58	82
11	6	39	60	7	47	72
12	4	32	54	5	38	65
13	2	28	48	4	34	58
14	1	24	42	3	29	50
15	–	20	38	2	24	46
16	–	18	33	2	22	40
17	–	15	28	1	18	34
18	–	14	26	1	16	31
19	–	11	23	1	13	28
20	–	10	21	–	12	25
21	–	9	19	–	11	23
22	–	7	18	–	8	22
23	–	6	16	–	7	19
24	–	5	14	–	6	17
25	–	4	12	–	5	14
26	–	4	11	–	5	13
27	–	3	10	–	4	12
28	–	3	10	–	4	11

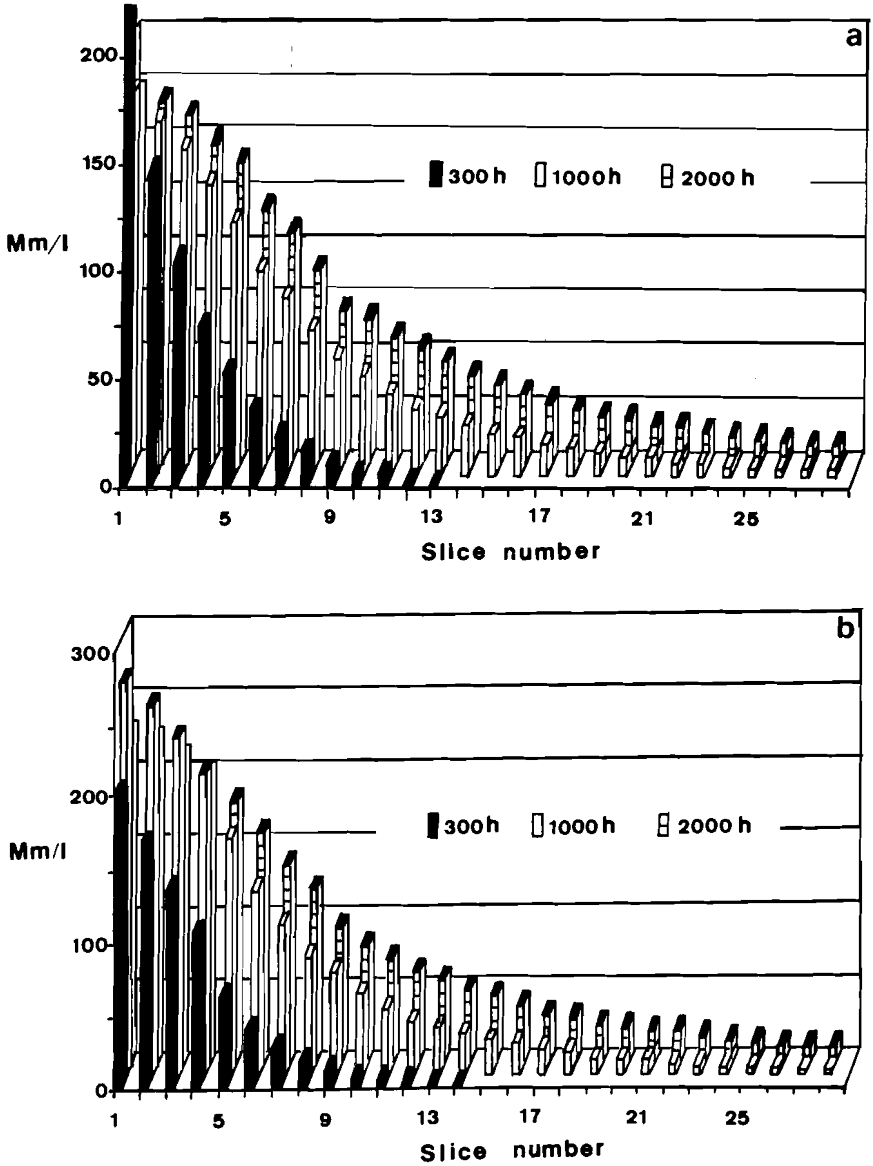

Fig. 2. Concentration profiles throughout the gel column. Mother solutions: (a) 0.5M $SrCl_2$; (b) 0.5M $BaCl_2$.

precludes the analytic treatment of the mass-transfer.

The knowledge of concentration evolution (space and time) allows us to calculate the reagent's diffusion constant for different diffusion times and locations in the gel column. With this object in mind, concentration data may be adjusted to writing known functions ($C = F(x, t)$). From these functions, diffusion constants may be obtained by applying Fick's second law. This objective is, however, beyond the scope of the present work. It is only worth noting here that the diffusion constants of the reagent change markedly throughout the gel column, as a consequence of concentration gradient. Later papers will deal with this matter.

A second aspect, the gel pH evolution, is turning out to be parallel to the mass-transfer phenomena. Fig. 3 shows the pH profile after 912 h of

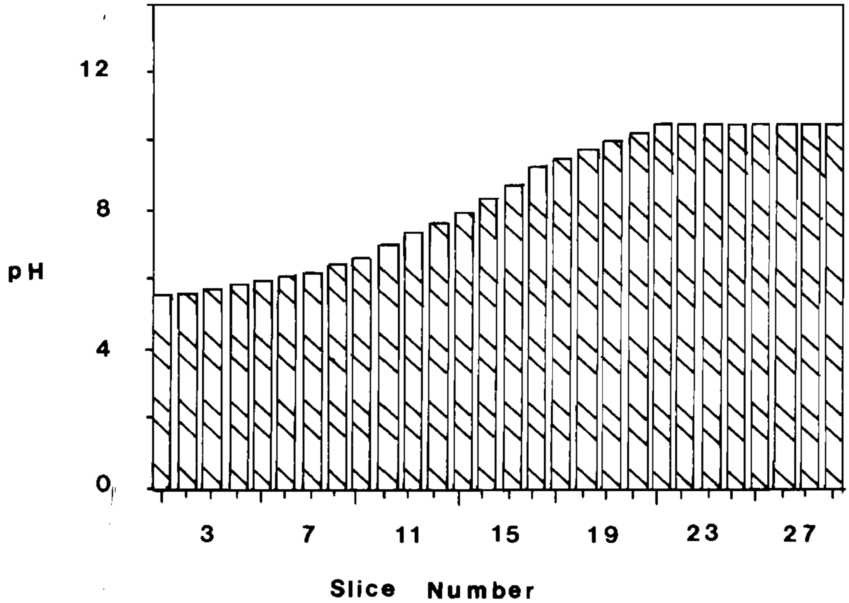

Fig. 3. pH profile after 912 h diffusion time. Mother solutions: (a) 0.5M $SrCl_2$; (b) 0.5N Na_2CO_3.

diffusion from 0.5M $SrCl_2$ and 0.5N Na_2CO_3 mother solutions. One can note that the pH increases from 5.5 in the slice 1 to 10.5 in the slice 21, and remains constant beyond this slice. The upward step is shifted from the carbonate reservoir extreme (slice 28) towards the further end, as diffusion time passes by. However, the whole shape of the pH profile remains the same.

According to these remarks, one would expect to find a parallelism between the pH and the total carbon concentration (species in solution in which such carbon is arranged will be considered later). Table 2 shows the values of the carbon total concentration and pH profiles throughout the gel column for different diffusion times. One can observe that the pH increases as the carbon concentration increases. Such an increase continues until the carbon concentration is about 35 mmoles/l and a pH 10.5 has been reached. Further concentration increases do not result in meaning pH changes.

The pH evolution must be considered necessarily in a rigorous treatment of crystal growth in gels. This evolution, as it is reported below, results in significant distribution changes of species (free ions and complexes) in solution, and, therefore, in the supersaturation profile throughout the gel column.

4. Species in solution and supersaturation throughout the gel column

For strontianite ($SrCO_3$) growth, the supersaturation can be written as follows:

$$\beta = \frac{a(\mathrm{Sr}^{2+})\,a(\mathrm{CO}_3^{2-})}{K_{\mathrm{sp}}}, \qquad (1)$$

where $a(\mathrm{Sr}^{2+})$ and $a(\mathrm{CO}_3^{2-})$ are the activities of the free ions in solution and K_{sp} is the thermodynamic solubility product ($K_{sp} = 10^{-9.03}$ at 25 °C).

Eq. (1) shows that the estimation of supersaturation requires knowledge of the free ion activities. Therefore, activity coefficients and concentration of Sr^{2+} and CO_3^{2-} free ions must be found.

For calculating the activity coefficients, the Debye–Hückel theory for moderately concentrated solutions may be used [6]. The application of the Debye–Hückel formula requires a calculation of the ionic strength of the solution, and this involves knowledge of the concentration of the various

Table 2
Total carbon concentration and pH profile throughout the gel column; mother solutions: 0.5M $SrCL_2$ and Na_2CO_3

Diffusion time: 500 h			Diffusion time: 1000 h		
Slice No.	pH	Total carbon (mM/l)	Slice No.	pH	Total carbon (mM/l)
1	5.5	13	1	5.5	14
2	5.5	13	2	5.5	14
3	5.5	13	3	5.5	14
4	5.5	13	4	6	15
5	5.5	13	5	6	15
6	5.5	13	6	6	15
7	5.5	13	7	6.5	16
8	5.5	13	8	6.5	16
9	5.5	14	9	7	17
10	5.5	14	10	7	17
11	6	15	11	7.5	18
12	6	15	12	8	19
13	6.5	16	13	8	19
14	6.5	16	14	8.5	20
15	7	17	15	9	22
16	7	17	16	9.5	24
17	7.5	18	17	10	25
18	8	19	18	10	28
19	8.5	20	19	10	31
20	9	22	20	10.5	36
21	9.5	24	21	10.5	41
22	10	28	22	10.5	47
23	10	34	23	10.5	54
24	10.5	46	24	10.5	61
25	10.5	60	25	10.5	71
26	10.5	69	26	10.5	75
27	10.5	81	27	10.5	80
28	10.5	95	28	10.5	84

species in solution. So, free ions as well as ionic associations resulting from short range interaction between neighbouring ions must be considered.

In the present case, the total concentrations of strontium, carbon, sodium and chlorine are known from the chemical analysis of gel slices, and pH measurement yields additional information. From these data the concentration of the relevant species (from a quantitative point of view) must be figured out. Such species are:

charged species: HCO_3^-, CO_3^{2-}, $NaCO_3^-$, Na^+, Sr^{2+}, OH^-, H^+, $SrOH^+$;
uncharged species: $H_2CO_3^0$, $NaHCO_3^0$, $NaOH^0$.

To calculate the concentration of these species, it is necessary to solve a system that is formed by the mass-balance equations and the equilibria of the different species in solution [7]. Such set of equations may be solved by a iterative procedure with the assistance of a microcomputer. The equilibrium constants may be obtained from the tables of Martell and Smith [8].

Finally, by solving this system, one can find the ionic strength and hence the activity coefficients and supersaturation.

An analogous method may be used to calculate the supersaturation in the case of witherite ($BaCO_3$) growth.

Fig. 4 shows the supersaturation profile for $SrCO_3$ when crystallization begins. Different initial concentrations of mother solutions are considered.

One may note that the supersaturation maximum is shifted towards the CO_3^{2-} reservoir. Analogous profiles may be observed for other initial concentrations of mother solutions.

A second aspect that one may point out is the high value reached by the supersaturation when the nucleation begins. Such an amount is larger than 3500 in some regions of the diffusion column. This means a high metastability level, which is to be expected for a system of limited particle mobility and for a substance with very low solubility.

In the case of witherite growth, the metastability field is smaller, since its solubility is higher ($K_{sp} = 10^{-8.3}$ at 25 ° C) than that of strontianite. The profile shapes are, however, similar. One can observe this point in fig. 5, which shows the witherite supersaturation profiles when crystallization begins.

With regard to supersaturation maximum locations, these are easily explainable by the distributions of the "carbon-containing" species, which is in its turn pH dependent. So, at a pH = 10.5, the contribution of HCO_3^- and $H_2CO_3^0$ to the total carbon concentration is low compared to that of CO_3^{2-}. On the contrary, at lower pH, HCO_3^- and $H_2CO_3^0$ are predominant.

Fig. 6 shows the concentration profiles of these species throughout the gel column. Such values correspond to the nucleation moment (912 h) in

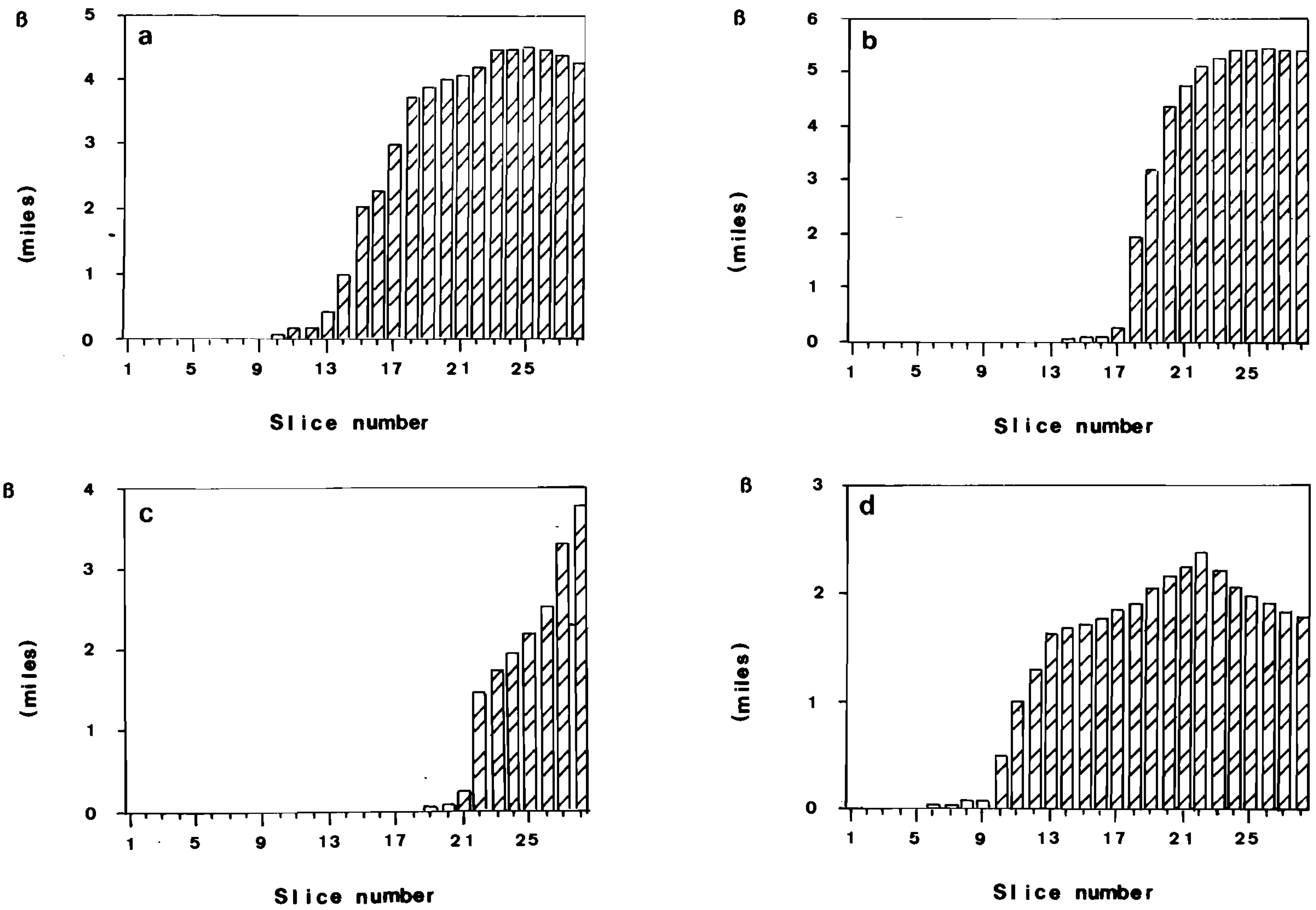

Fig. 4. Strontianite supersaturation profiles at the nucleation time. Concentration of $SrCl_2$ and Na_2CO_3 mother solutions: (a) 0.5M and 0.5N; (b) 0.5M and 0.3N; (c) 0.5M and 0.1N; (d) 0.1M and 0.5N.

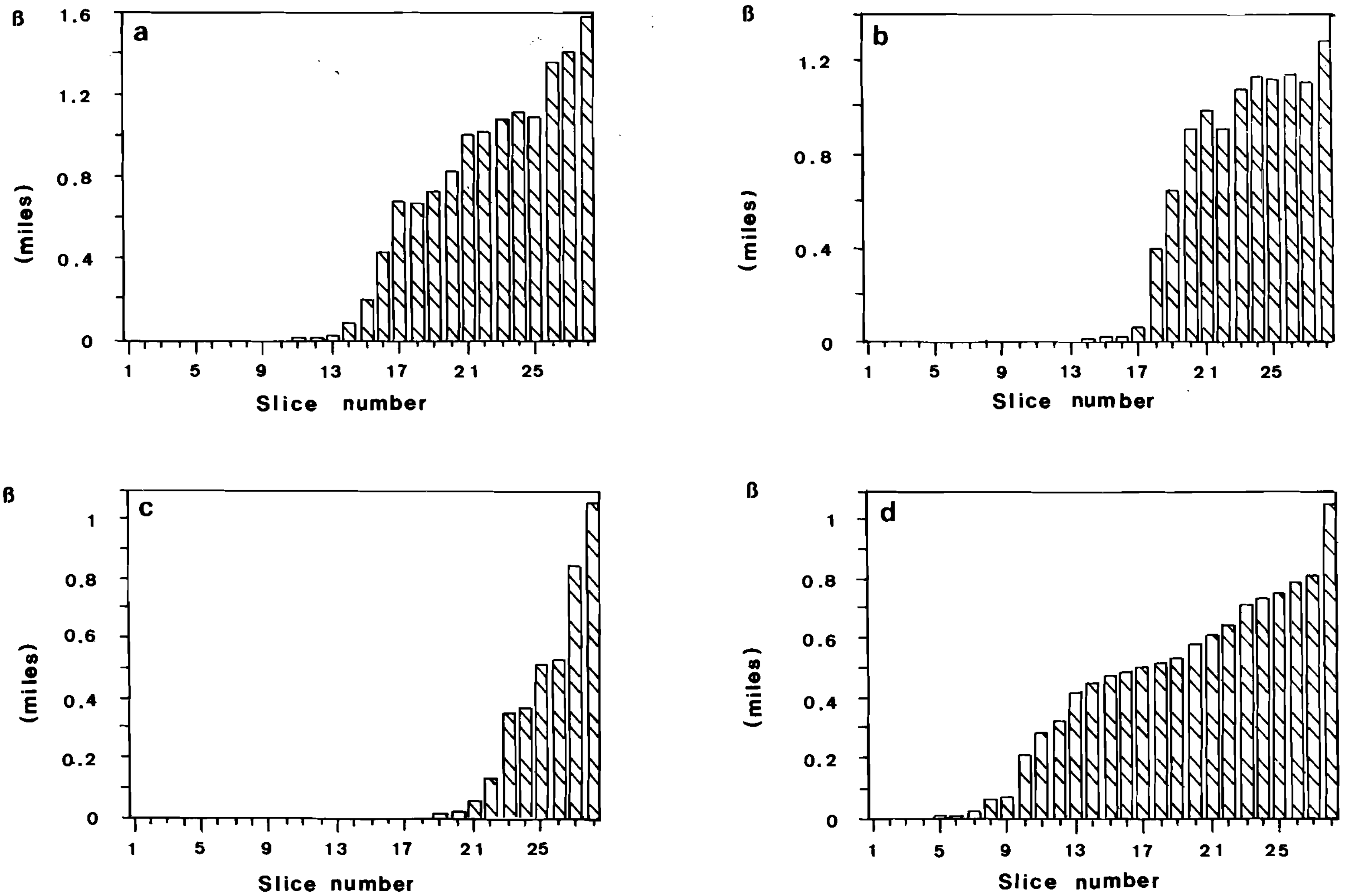

Fig. 5. Witherite supersaturation profiles at the nucleation time. Concentration of $BaCl_2$ and Na_2CO_3 mother solutions: (a) 0.5M and 0.5N; (b) 0.5M and 0.3N; (c) 0.5M and 0.1N; (d) 0.1M and 0.5N.

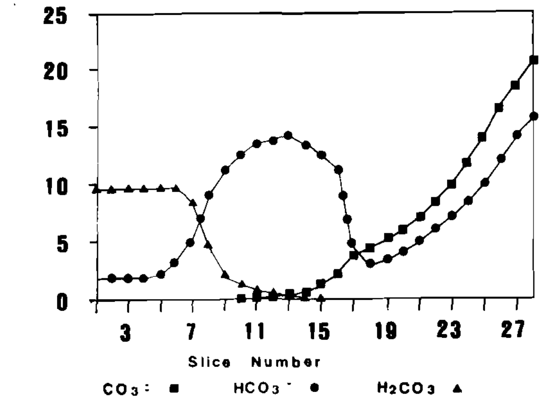

Fig. 6. Concentration profiles of "carbon-containing" species throughout the gel column. Diffusion time: 912 h. Mother solutions: 0.5M $SrCl_2$ and 0.5N Na_2CO_3.

the case of 0.5M $SrCl_2$ and 0.5N Na_2CO_3 mother solutions. Fig. 3, reported before, shows the respective pH profile.

From these figures, one may note that for low total carbon concentration, the low pH (5.5) involves the fact that $H_2CO_3^0$ is the prevailing species (slices 1–7). As carbon concentration (and pH) increases, HCO_3^- becomes predominant (slices 7–16), and finally, CO_3^{2-} is the most abundant specie is slices 16 to 28.

It is also worth noting that $NaHCO_3^0$ and $NaCO_3^-$ are very abundant ionic associations. This is a consequence of the high sodium concentration in the system, since the preparation of silica gel involves formation of NaCl as a soluble by-product.

According to these statements, the CO_3^{2-} concentration is only of importance, in the nearest tube half to the Na_2CO_3 reservoir. This explains that the maximum supersaturation values are constrained to this region of the system.

5. Growth mechanism and crystallization criteria

For studying nucleation and growth behaviour of $SrCO_3$ and $BaCO_3$, crystal growth experiments have been carried out. Different concentrations of mother solutions have been used. Nucleation density, experimental induction time and first crystallization location are reported in table 3.

In the early growth stages, strontianite crystals show dendritic shapes with curved and rough surfaces (fig.7). Such morphologies involve a continuous growth mechanism, which is characteristic of interfaces with high kinetic roughness [9]. Such a roughness is easily explainable by the high supersaturation level in this stage.

Afterwards, as a result of the growth process, the supersaturation decays in such a way that strontianite crystals enter into the growth region where the growth rate is controlled by two-dimensional nucleation or spiral growth mechanisms. This leads to a progressive development of the dendritic aggregate individuals that become singular-faceted. Such individual crystallites are formed by rhombic prism faces or aragonite-type twins (fig. 8).

One can observe an analogous morphological evolution in the witherite growth, but in this case the continuous growth mechanism leads to split

Table 3
Nucleation density, experimental induction time and first precipitate location for strontianite and witherite growth in gels; diffusion path: 280 mm

Mother solutions		Induction time (h)	Precipitate location (slices)	Number of nuclei
Sr–Ba	Na_2CO_3			
Strontianite				
0.5M	0.5N	912	17–21	14
0.5M	0.3N	1200	19–23	12
0.5M	0.1N	1344	23–27	9
0.3M	0.5N	1080	16–18	10
0.3M	0.3N	1200	18–21	4
0.3M	0.1N	1440	22–24	3
0.1M	0.5N	1344	14–17	6
0.1M	0.3N	1588	17–19	3
0.1M	0.1N	1632	19–20	2
Witherite				
0.5M	0.5N	864	18–22	4
0.5M	0.3N	1128	19–24	4
0.5M	0.1N	1344	24–26	2
0.3M	0.5N	1080	16–19	4
0.3M	0.3N	1200	17–20	4
0.3M	0.1N	1464	20–22	2
0.1M	0.5N	1392	16–18	3
0.1M	0.3N	1536	18–20	2
0.1M	0.1N	1704	19–21	2

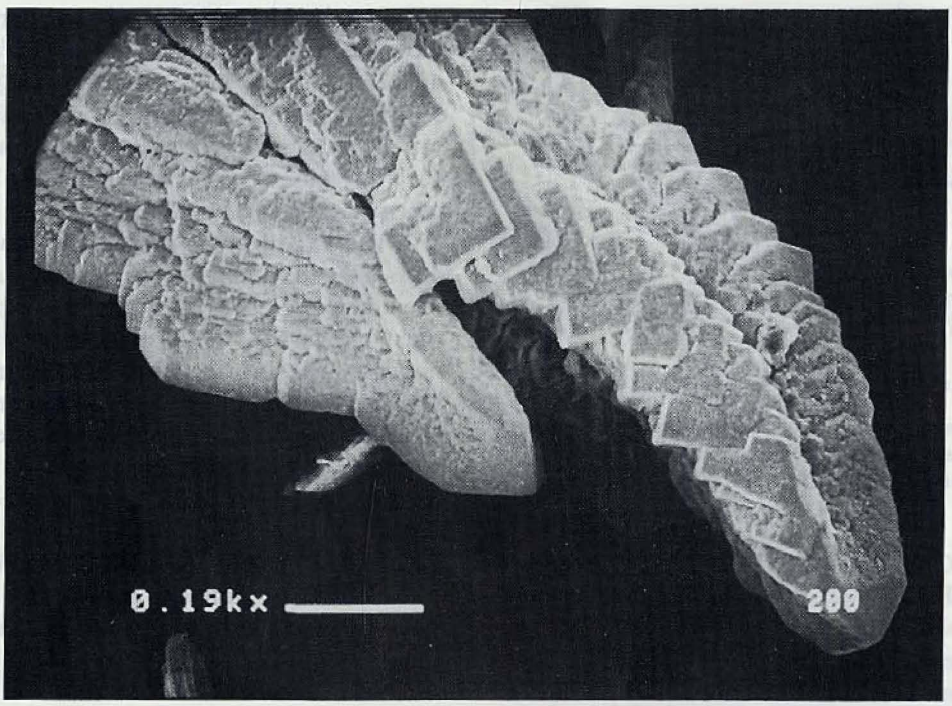

Fig. 7. Strontianite dendrites.

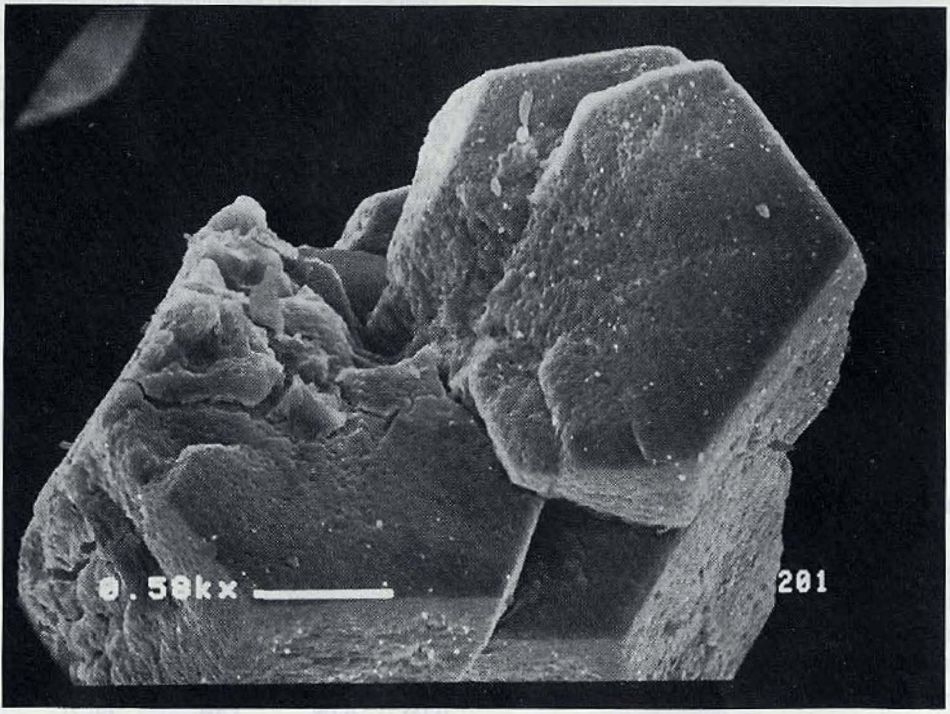

Fig. 8. Pseudohexagonal individual crystallites of strontianite.

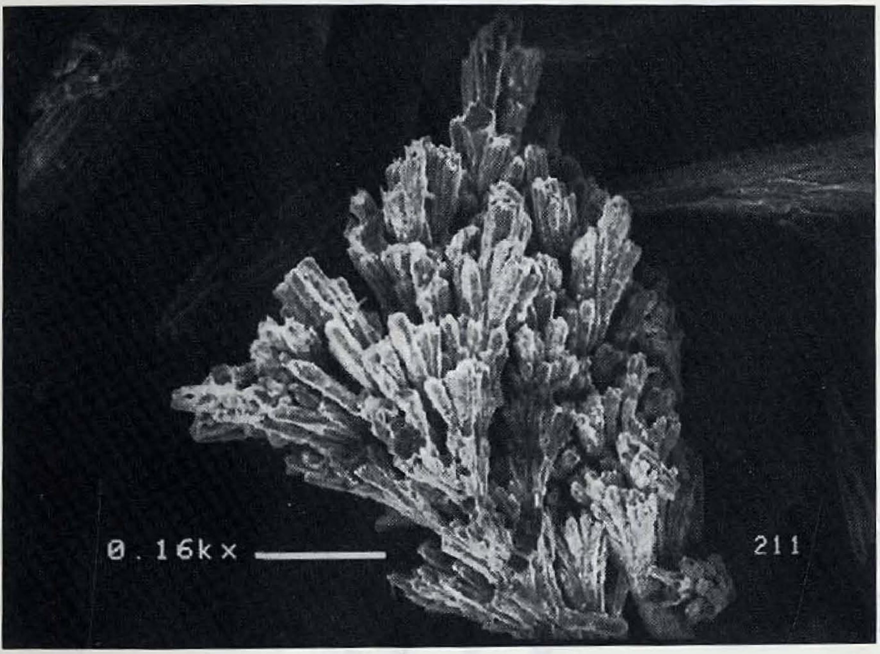

Fig. 9. Witherite split growth.

growth shapes (fig. 9). Then, as supersaturation decreases, individuals become singular-faceted.

Although no difference between growth morphologies exists, different mother solution concentrations lead to different nucleation densities. Such a phenomenon may be explained by the supersaturation rate ($\delta\beta/\delta t$), which depends in its turn on the initial concentration of the reagent. A systematic study of supersaturation rate evolution is, however, beyond the scope of the present work.

Table 3 also shows time and location of the first precipitates. These data are undoubtedly the most outstanding for the theory of crystal growth in diffusing-reacting systems. In fact, precipitate location data may be used to find rigorous crystallization criteria. With this aim, such data must be confronted with the concentration and supersaturation profiles.

One can observe that the first precipitate location does not agrees with the supersaturation maximum. Following Henisch and García-Ruiz [1], this means that the critical supersaturation condition is an insuficient requisite to begin the nucleation. Although the critical supersaturation condition remains necessary, a complementary hypothesis has to be introduced to account for observations. In this way, the knowledge of concentration profiles is important to check if the "equality range" condition is fulfilled.

Fig. 10 shows the Sr^{2+} and CO_3^{2-} concentration profiles when crystallization begins. Different initial concentrations are considered. The first precipitate locations are outlined in the upper part of the graphics. Analogous graphics are shown in fig. 11 for $BaCO_3$ growth.

Figs. 10 and 11 demonstrate that the nucleation zone is constrained to a limited range of concentration ratios. The nucleation probability tends to zero rather rapidly as the $[CO_3^{2-}]/[Sr^{2+}]$ or $[CO_3^{2-}]/[Ba^{2+}]$ ratios depart significantly from unity. Therefore the equality range is a complementary hypothesis that explains the experimental results shown here. Such a condition is fulfilled for both sustances and for all the initial concentrations used here.

Consequently, the behaviour of the described gel-diffusion systems is correctly reproduced by a dual condition: equality range and critical super-

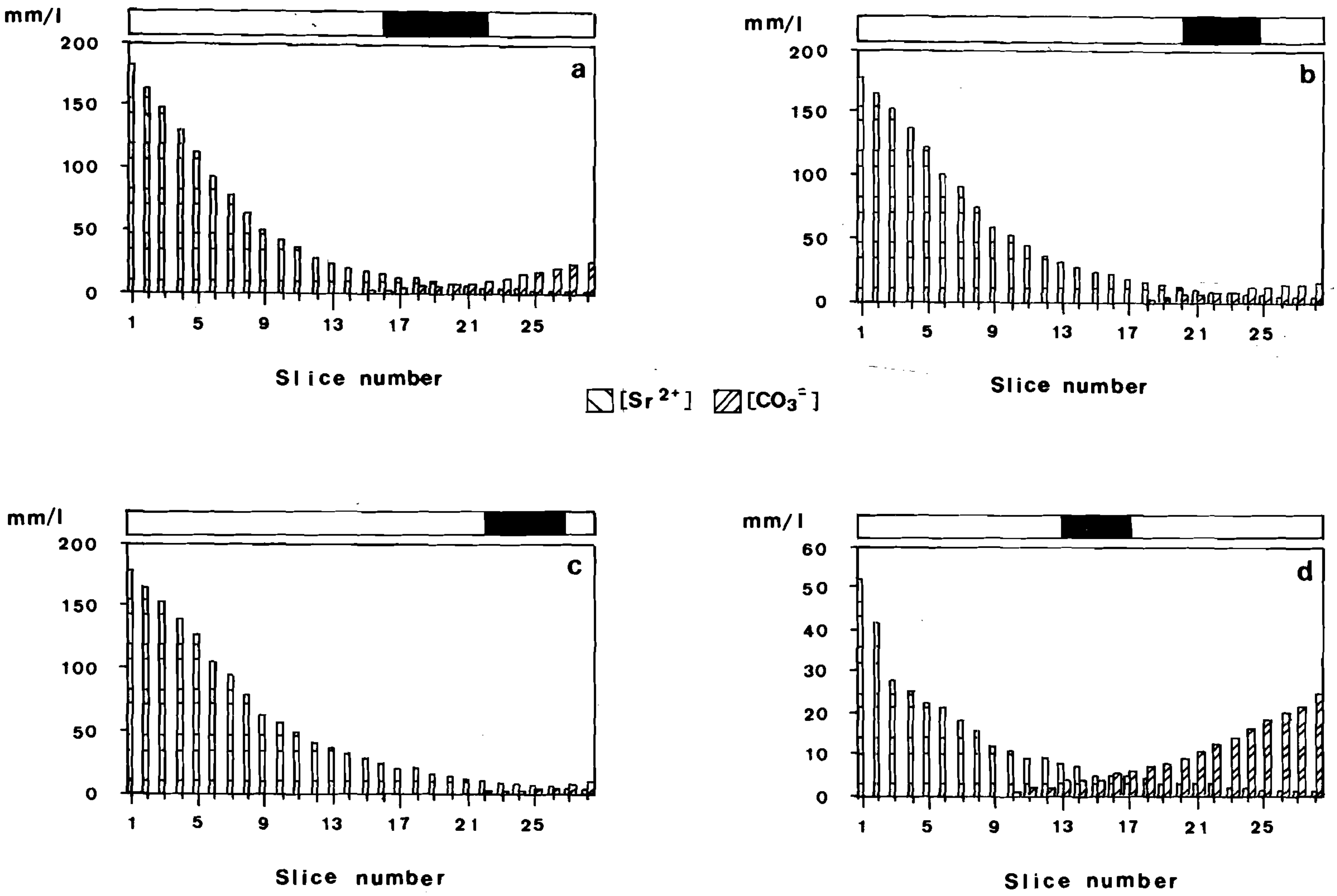

Fig. 10. Sr^{2+} and CO_3^{2-} concentration profiles at the strontianite nucleation time. The reaction zone is outlined in the upper part of the graphics. Concentration of $SrCl_2$ and Na_2CO_3 mother solutions: (a) 0.5M and 0.5N; (b) 0.5M and 0.3N; (c) 0.5M and 0.1N; (d) 0.1M and 0.5N.

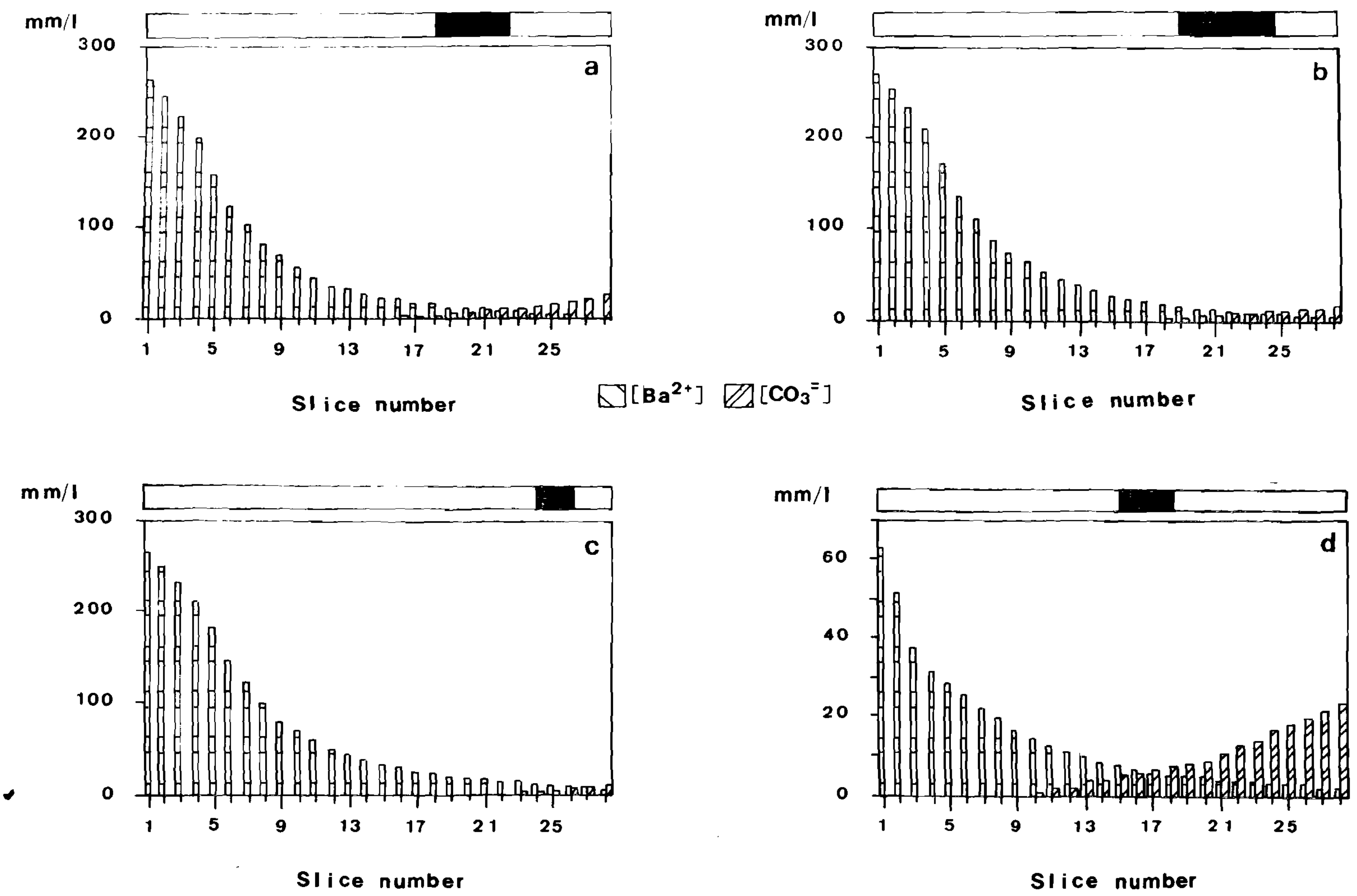

Fig. 11. Ba^{2+} and CO_3^{2-} concentration profiles at the whitherite nucleation time. The reaction zone is outlined in the upper part of the graphics. Concentration of $BaCl_2$ and Na_2CO_3 mother solutions: (a) 0.5M and 0.5N; (b) 0.5M and 0.3N; (c) 0.5M and 0.1N; (d) 0.1M and 0.5N.

saturation requisites must be simultaneously fulfilled.

6. Summary

The experimental testing of both mass-transfer and pH evolution is the background to establish rigorous hypotheses to explain nucleation and growth behaviour in crystal growth in gels. The pH evolution results in significant distribution changes of species in solution, and therefore in the supersaturation and concentration profiles throughout the gel column.

Experimental results demonstrate that, contrary to frequently made assumptions, the critical supersaturation condition is insufficient to account for nucleation behaviour. In the case of strontianite and witherite nucleation, a second condition – the "equality range" of reagent concentrations – must be fulfilled.

Acknowledgments

This work was done as a part of project No. 472/84 supported by CAICYT (Ministry of Education and Science of Spain). The authors gratefully acknowledge the help of Dra. P. Cubas for the SEM work. The authors are also indebted to the Laboratorio de Mineralogía y Edafología, Universidad Castilla–La Mancha, for the C–N–S analysis.

References

[1] H.K. Henisch and J.M. García-Ruiz, J. Crystal Growth 75 (1986) 195.

[2] M. Prieto, C. Viedma, V. López-Acevedo, J.L. Martín-Vivaldi and S. López-Andrés, J. Crystal Growth 92 (1988) 61.

[3] D. Srzić, B. Pokrić and Z. Pučar, Z. Physik. Chem. 103 (1976) 157.

[4] H.K. Henisch and J.M. García-Ruiz, J. Crystal Growth 75 (1986) 203.

[5] A.G. Walton, in: Nucleation, Ed. A.C. Zettlemoyer (Dekker, New York, 1969).

[6] C. van Leeuwen and L.J.M.J. Blomen, J. Crystal Growth 46 (1979) 96.

[7] H.E. Lundager Madsen, Nephrologie 5 (1985) 151.

[8] A.M. Martell and R.M. Smith, Critical Stability Constants (Plenum, New York, 1974).

[9] I. Sunagawa, Bull. Mineral. 104 (1981) 81.